JOURNAL OF EXPERIMENTAL ZOOLOGY 303A:880–893 (2005)

Adaptation to Hypoosmotic Challenge in Brachyuran Crabs: A Microanatomical and Electrophysiological Characterization of the Intestinal Epithelia

JOHN CAMPBELL McNAMARA[1]*, FLAVIA P. ZANOTTO[1,2], AND HORST ONKEN[3]
[1]*Departamento de Biologia, Faculdade de Filosofia, Ciências e Letras de Ribeirão Preto, Universidade de São Paulo, Avenida Bandeirantes 3900, Ribeirão Preto 14040-901, SP, Brasil*
[2]*Departamento de Fisiologia, Instituto de Biociências, Universidade de São Paulo, Cidade Universitária, Rua do Matão, Travessa 14, 101, São Paulo 05508-900, SP, Brasil*
[3]*School of Biological Sciences, Washington State University, Pullman, Washington 99164-4236*

ABSTRACT Besides its role in digestion and nutrient absorption, the crustacean gut participates in osmo/ionic regulation. We investigate microanatomy, ionic permeability and transepithelial electrophysiological parameters in the mid- and hindguts of three hyperosmoregulating crabs that inhabit estuarine waters (*Chasmagnathus granulata*), brackish mangrove swamp (*Sesarma rectum*) or freshwater (*Dilocarcinus pagei*). The abdominal hindguts are cuticle lined, the single-layered epithelia consisting of narrow, columnar cells exhibiting apically dense, unvesiculated cytoplasm. In the saltwater species, the thoracic midgut epithelium consists of tall, narrow, columnar cells displaying numerous, apical microvilli above dense apical cytoplasm. However, the corresponding gut segment in the hololimnetic species, *D. pagei*, consists of squat cells lacking apical microvilli, overlain by a heavy cuticle, constituting a thoracic or anterior hindgut. The midgut/thoracic hindgut epithelia in all three crabs, and abdominal (posterior) hindgut of *D. pagei*, exhibit similar, small, lumen-negative voltages when perfused symmetrically with hemolymph-like salines. The hindguts of the saltwater species show similar, small, lumen-positive voltages. Small short-circuit currents are detectable after voltage clamping. Washout and/or addition of luminal glucose or amino acids do not alter current or conductance, suggesting the absence of active, electrogenic nutrient absorption. Ion substitution did not disclose active, electrogenic absorption or secretion of Na^+ and/or Cl^-. The midguts of the saltwater species exhibit similar conductances, greater than in *D. pagei*, but no ion selectivity; hindgut conductance is low, the epithelia showing moderate anion selectivity. The thoracic (anterior) and abdominal (posterior) hindgut epithelia of *D. pagei*, the freshwater species, exhibit similar, low conductances, and are ion selective. These findings reveal that active, electrogenic, salt and nutrient transport is undetectably low or absent. The reduced transepithelial conductances and notable ion selectivities in the abdominal and thoracic hindguts of *D. pagei* may reduce passive salt losses in fresh water, contributing to osmotic and ionic regulation. *J. Exp. Zool. 303A:880–893, 2005.*

Grant sponsor: Fundação de Amparo à Pesquisa do Estado de São Paulo, Brazil; Grant number: FAPESP no. 1998/09756-9; Grant sponsor: Deutscher Akademischer Austauschdienst (DAAD/GTZ) Germany; Grant sponsor: Visiting Professorship from CAPES(Brazil)/DAAD; Grant sponsor: Research scholarship from the Conselho Nacional de Desenvolvimento Científico e Tecnológico; Grant number: CNPq no. 303282/84-3
*Correspondence to: John C. McNamara, Departamento de Biologia, FFCLRP, Universidade de São Paulo, Ribeirão Preto 14040-902, SP, Brasil. E-mail: mcnamara@ffclrp.usp.br
Present address: Flavia P. Zanotto, Universidade Presbiteriana Mackenzie, Faculdade de Ciências Biológicas Exatas e Experimentais, Rua da Consolação 930, São Paulo 01302-907, SP, Brasil.
Received 7 August 2004; Accepted 7 May 2005
Published online in Wiley InterScience (www.interscience.wiley.com). DOI: 10.1002/jez.a.216.

While nutrition in the Crustacea is well studied, most reports have focused on economically important decapods like shrimps, lobsters and freshwater prawns (see review by Cuzon et al., '94; Mu et al., '98). In contrast, the nutritional requirements of brachyuran crabs are poorly known (see review by Zanotto, 2000), as is the physiology of nutrient uptake by their digestive systems.

In the Crustacea, the gut is essentially a simple tube running the length of the body, differentiated into foregut, midgut and hindgut (Dall and Moriarty, '83; Herrera-Alvarez et al., 2000). The foregut and hindgut are lined by cuticle, and derive from the embryonic ectoderm. However, the midgut, originating in the embryonic endoderm, has no cuticle, and the apical microvilli of its epithelial cells make direct contact with the gut lumen. The crustacean digestive system also includes the midgut gland or hepatopancreas, and ceca and diverticula; considerable diversity is apparent in the morphology and complexity of these ancillary regions (Icely and Nott, '92; Brunet et al., '94).

Thus far, intestinal transport in the Crustacea has been studied at the whole animal level, or in physiological preparations of isolated, perfused gut segments (Ahearn and Maginniss, '77; Ahearn, '78, '80), and at the cellular level, using plasma membrane vesicles from lobster hepatopancreas but not midgut specifically (Ahearn et al., '85, '86; Chu, '87; Ahearn, '96). A role for the midgut in both nutrient absorption and osmoregulation in the Crustacea is still controversial. While early works suggested an absorptive role for the midgut (Yonge, '24), recent studies reveal that nutrient absorption takes place via the hepatopancreas (Ahearn, '85, '86, '96, '99). Further, the gills and antennal glands are undoubtedly the main osmoregulatory effectors (Mantel and Farmer, '83; Ahearn and Franco, '90, '93; Lucu, '93; Flik et al., '94; Onken and McNamara, 2000). In contrast, in other arthropods like insects, the midgut exhibits very distinct ion transporting properties, critical to maintaining appropriate ionic concentrations and the alkaline pH typical of digestion in this group (Dow, '81; Clark et al., 2000). Mykles ('79) suggests that the ultrastructure of the midgut and hindgut in many Crustacea is indicative of a transport function. Thus, whether the decapod crustacean gut plays a role in osmoregulation besides nutrient uptake requires more thorough investigation.

Chu ('87), performing electrophysiological measurements on gut preparations, recorded very reduced transmural potential differences in the mid- and hindguts of the blue crab, *Callinectes sapidus*. This potential difference was unaffected by low salinity acclimation, suggesting that active Na^+ absorption by the midgut may be of limited importance in Na^+ hyperregulation. However, changes in passive Na^+ permeability are reduced in crabs acclimated to reduced salinities (Chu, '87). In the freshwater prawn, *Macrobrachium rosenbergii*, the midgut functions in ionic regulation and nutrient uptake (Ahearn and Maginniss, '77; Ahearn, '78, '80), specifically in glucose absorption (Ahearn and Maginniss, '77), which is apparently facilitated by Na^+ and Cl^- transport. Further, Ca^{2+} is co-transported with other ions across the apical membrane of the midgut cells (Ahearn, '78), resulting in an electrical potential difference across this epithelium (Ahearn, '80). Amino acid absorption apparently occurs in marine shrimps (Ahearn, '74, '76).

To our knowledge, crustacean intestinal epithelia have not been studied using micro Ussing-type chambers, a method sufficiently sensitive to detect transport phenomena in such preparations. The present comparative study combines this electrophysiological approach, accompanied by an estimation of epithelial ionic permeabilities based on conductance measurements, with a micro-anatomical characterization of the mid- and hindgut regions of three crab species from habitats presenting different osmotic challenges. The estuarine crab, *Chasmagnathus granulata*, is a strong hyper–hypoosmoregulator that inhabits saline media ranging from 1‰ to 30‰ salinity (S) (D'Incao et al., '92); the semi-terrestrial, amphibious crab, *Sesarma rectum*, habits mangrove swamps with a salinity of around 16‰ S (personal observations); and *Dilocarcinus pagei*, a true, freshwater crab encountered in inland waters (<0.5‰ S), is a strong hyperosmoregulator (Onken and McNamara, 2002).

We thus evaluate whether the mid- and hindguts might play a role in osmoregulation and nutrient uptake via active, electrogenic transport, and attempt to correlate observable differences in ionic permeability and microanatomy with the differential osmotic challenges confronted by these various crab species.

MATERIALS AND METHODS

Animals

C. granulata were obtained from Lagoa dos Patos, Rio Grande do Sul State, Brazil. *S. rectum*

were collected from the Itaguaré estuary near Bertioga (23°47.716′S, 46°03.327′W), and *D. pagei* from the Mogi-Guaçu River (21°12.143′S, 48°10.300′W), both in São Paulo State, Brazil. In the laboratory, the crabs were held in tanks containing either aerated, dilute seawater (*C. granulata*, 2‰ S; *S. rectum*, 15‰ S) or freshwater (*D. pagei*, <0.5‰ S), where they had free access to a dry surface. *C. granulata* were fed three times a week with minced meat, *S. rectum* with mangrove leaves, and *D. pagei* with lettuce, carrot or shrimp abdomens.

Salines

Hemolymph-like salines for *D. pagei* were prepared according to Onken and McNamara (2002); those for *C. granulata* were based on data from Bromberg et al. ('95). The salines for *S. rectum* were based on measured hemolymph osmolality ($746 \pm 44.3\,\mathrm{mOsm\,kg^{-1}}$) and ionic concentrations (Na^+ 246 ± 8.6, K^+ 11 ± 1.2, Ca^{2+} 13.6 ± 1.1, Cl^- $338 \pm 12.2\,\mathrm{mmol\,l^{-1}}$). All values are in $\mathrm{mmol\,l^{-1}}$: *S. rectum*, NaCl 250, $NaHCO_3$ 2, KCl 10, $CaCl_2$ 14, $MgCl_2$ 10, glucose 5, HEPES 5, pH 7.6; *C. granulata*, NaCl 335, Na^+-gluconate 50, $NaHCO_3$ 2, K^+-gluconate 6, Ca^{2+}-gluconate 8, Mg^{2+}-gluconate 3, glucose 5, HEPES 5, pH 7.6; *D. pagei*, NaCl 200, $NaHCO_3$ 2, KCl 5, $CaCl_2$ 10, glucose 5, HEPES 5, pH 7.6.

In the Na^+-free salines, choline chloride was substituted for NaCl, $KHCO_3$ for $NaHCO_3$ (reduced KCl), and *N*-methylglucamine sulfate for Na^+-gluconate. In the Cl^--free salines, gluconates substituted for the chlorides. NaCl-free salines were prepared with *N*-methylglucamine sulfate, $KHCO_3$ and K^+, Ca^{2+}, and Mg^{2+} gluconates. Sucrose was used to compensate the decrease in osmolality owing to *N*-methylglucamine sulfate substitution. In some experiments, glucose-free salines were employed, or $1\,\mathrm{mmol\,l^{-1}}$ arginine, lysine or valine was added. The salts used were obtained from Sigma (Munich, Germany), Fluka (Seelze, Germany), Roth (Karlsruhe, Germany) or Labsynth (Diadema, Brazil).

Physiological preparations

The crabs were anesthetized by immersion in crushed ice for about 10 min before killing by rapidly destroying the cerebral and thoracic ganglia with scissors. The carapace was carefully opened and the dorsal heart, gills and part of the hepatopancreas were removed prior to dorsally dissecting a short segment of the tubular midgut in the posterior thoracic region.

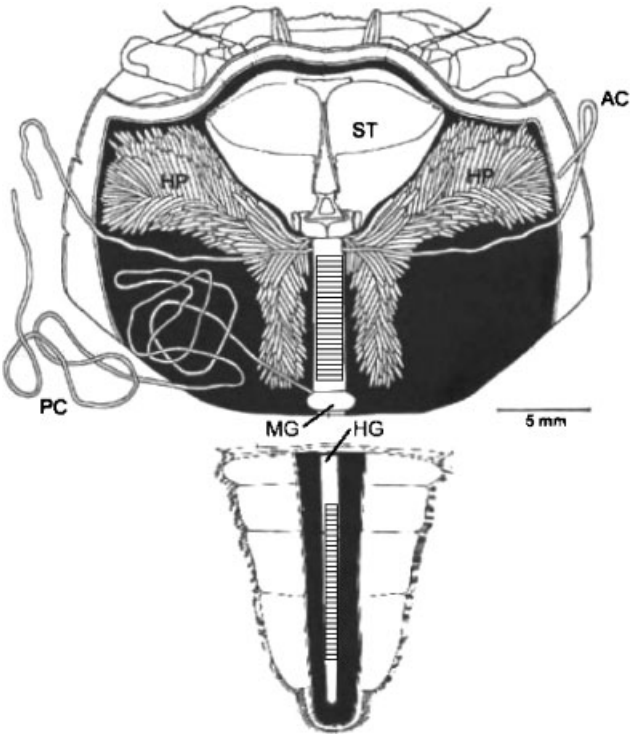

Fig. 1. Typical brachyuran digestive system, with locations of the gut segments used (hatched regions). AC, anterior cecum; HG, hindgut; HP, hepatopancreas; MG, midgut; PC, posterior cecum; ST, stomach (modified from Bond-Buckup et al., '91).

The abdomen was separated, opened ventrally and a median segment of hindgut dissected. The locations from which the isolated gut segments were obtained are given in Figure 1. The preparations were placed in their respective hemolymph-like salines until use in the electrophysiological or microscopical studies.

Microscopical studies

Mid- and hindgut preparations from each crab species were dissected as above and fixed on ice for 2 hr in a fixative consisting of $300\,\mathrm{mmol\,l^{-1}}$ paraformaldehyde and $250\,\mathrm{mmol\,l^{-1}}$ glutaraldehyde in $100\,\mathrm{mmol\,l^{-1}}$ Na^+ cacodylate buffer (pH 7.4), containing ($\mathrm{mmol\,l^{-1}}$) Na^+ 250, K^+ 10, Ca^{2+} 15 and Mg^{2+} 10 as chlorides. The gut samples were then rinsed in buffer alone, further dissected and post-fixed for 1.5 hr in buffered 2% OsO_4.

For light microscopy, tissue blocks were routinely dehydrated in a graded ethanol series followed by propylene oxide, embedded in Araldite 502 resin, sectioned at 0.5 μm thickness on a Leica Ultracut-R ultramicrotome, and stained with 1%

methylene/toluidine blue in 1% aqueous borax. Sections were photographed at 200–400× employing digital imaging using a Zeiss Axiophot microscope and Zeiss AxioVision 3 image acquisition software.

For scanning electron microscopy, samples were critical point dried (Baltec CPD 030) in amyl acetate/liquid CO_2, sputter coated with 30 nm gold (Baltec SCD 050) and observed at 500–3000× in a Jeol 5200 scanning electron microscope. Micrographs were digitized directly from the negatives.

Electrophysiological studies

For electrophysiological experiments, the gut segments were opened and mounted in a micro Ussing-type chamber. To minimize edge damage, silicon grease and a rubber O-ring were used. Epithelial surfaces of 0.02 cm^2 were exposed to the internal and external compartments (50 µl volume each) and gravity-perfused continuously with aerated saline (approximately 2 ml min^{-1}). For voltage measurements, calomel electrodes were connected via agar bridges (3% agar in 3 mol l^{-1} KCl) to both sides of the preparation, the distance from the bridge tip to the tissue being <1 mm. The reference electrode was placed in the internal bath. AgCl-coated silver wires served as electrodes to apply current for short-circuiting (i.e., measurement of the short-circuit current, I_{sc}) through an automatic clamping device (Model VCC 600, Physiologic Instruments, San Diego, CA). The preparation conductance (G_{te}) was calculated from imposed voltage pulses (ΔV) and the resulting current deflections (ΔI). The data were registered continuously on a chart recorder (Type 3229 I/85, Linseis, Selb, Germany).

Ionic permeabilities were estimated from changes in I_{sc} and G_{te} after adding salts (Na^+, K^+, Ca^{2+} and Mg^{2+} as gluconates; Mg^{2+} as Cl^-; NO_3^-, CH_3COO^- and SO_4^{2-}) to the external, NaCl-free saline. When addition of one of the salts produced no (or negligible) change in I_{sc}, anions and cations were assumed to contribute 50% each to the resulting change in G_{te}. The specific conductances of all ions (G_x) could then be measured, and the absolute permeabilities (P_x) were calculated according to Hodgkin and Horowitz ('59) from the equation

$$P_x = \frac{\Delta G_x}{a_x} \times \frac{R \times T}{z^2 \times F^2} [\text{cm} \times \text{s}^{-1}],$$

where R, T, F and z have their usual values, and a_x is the ionic activity, that is, the product of the concentration and the activity coefficient (f_x). Values of f_x were estimated by measuring the osmolalities of the single salt solutions and were as follows: Na^+-gluconate 0.91, K^+-gluconate 0.98, Ca^{2+}-gluconate 0.61, Mg^{2+}-gluconate 0.66, $MgCl_2$ 0.79, $Mg(NO_3)_2$ 0.83, Mg^{2+}-acetate 0.89 and $MgSO_4$ 0.63. Final values for transepithelial voltage (V_{te}), short-circuit current (I_{sc}), transepithelial conductance (G_{te}) and ion permeability (P_x) are given in the results as the mean ± standard error of the mean (SEM).

Statistical analyses

Electrophysiological data were analyzed using a one-way ANOVA/Student–Newman–Keuls multiple means procedure to verify a species effect and locate significant differences. Hindgut and midgut data were compared using unpaired *t*-tests. Effects and differences were considered significant at $P = 0.05$ (SigmaStat v2.03 software, SPSS Inc., Chicago, IL).

RESULTS

The mangrove crab, Sesarma rectum, adapted to 15‰ salinity

Micro-anatomy

In *S. rectum*, the lightly folded midgut epithelium (Fig. 2A) is about 80 µm thick, and consists predominantly of a single layer of tall, narrow, columnar cells sitting on a dense, undulating basement membrane, underlain by a 40-µm-thick basement lamina comprising smooth muscle blocks lying in a fibrous parenchyma penetrated by blood vessels. The luminal surface of the columnar cells exhibits prominent microvilli above a very dense layer of cytoplasm. The upper two-thirds of the cytoplasm is heavily vesiculated and contains the lightly staining, medial, elliptical nucleus; the lower third is filled with a dense, finely tubular reticulum. Occasional basal cells with a small, dense, irregular nucleus lie close to the basement membrane between the columnar cells.

The hindgut epithelium, of some 40-µm thickness (Fig. 2B), is overlain by a heavy, 20-µm-thick cuticle, and consists mainly of narrow, dense, columnar cells that interdigitate with lighter, infrequent, large globular cells, sitting on an indistinct basal membrane underlain by a thick, fibrous basal lamina. The columnar cell cytoplasm is unvesiculated and harbors an elliptical, mainly medially located nucleus; the upper apical cytoplasm is notably dense. The globular cells are

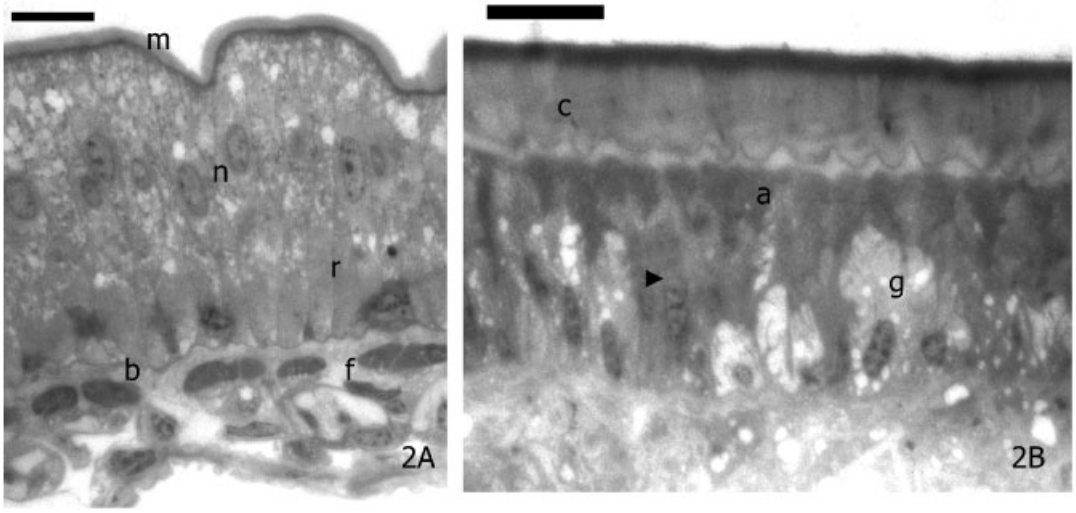

Fig. 2. Micro-anatomy of the mid- and hindguts of the mangrove crab, *Sesarma rectum*, adapted to 15‰ salinity. (**A**) Transverse section through the midgut wall revealing the homogeneous layer of tall, columnar epithelial cells exhibiting apical microvilli (m), medially located nuclei (n) and basal reticulum (r), overlying the basement membrane (b) and bundles of longitudinal muscle fibers (f). (**B**) Transverse section through the hindgut showing the thick cuticle (c) above an epithelium consisting of columnar cells (arrowhead) with dense apical cytoplasm (a) and medial nuclei, and globular, lighter staining, vesicle-containing cells (g) with basal nuclei. Scale bars = 20 μm.

vesiculated with a basal nucleus, and may constitute part of the cuticle-secreting tegumental glands.

Electrophysiology

After mounting the opened midgut tissue sheet from *S. rectum*, a transepithelial voltage (V_{te}) of -0.3 ± 0.2 mV ($N = 3$) was recorded on symmetrically perfusing the preparation with hemolymph-like NaCl saline. Short-circuiting V_{te} resulted in a short-circuit current (I_{sc}) of $+16 \pm 12\,\mu A\,cm^{-2}$ with a transepithelial conductance (G_{te}) of $58 \pm 9\,mS\,cm^{-2}$. Omission of external glucose did not affect I_{sc} or G_{te}. Similarly, the addition of external arginine, lysine or valine ($1\,mmol\,l^{-1}$) did not alter these parameters. When Na^+- or Cl^--free salines were perfused on both sides of the preparation to disclose putative, internal short-circuiting of active Na^+ and Cl^- absorption/secretion, no significant short-circuit currents reflecting active ion transport were found.

The ionic permeabilities of this midgut tissue are summarized in Figure 3. The mean permeability sequence established was $Cl^- \cong K^+ > Na^+ \cong NO_3^- > CH_3COO^- > SO_4^{2-} \cong$ gluconate $> Ca^{2+} \cong Mg^{2+}$. The ratio between the permeabilities of the most abundant anion and cation ($P_{Cl^-}:P_{Na^+} = 1.3$) reveals the absence of significant anion or cation selectivities.

Hindgut tissue, perfused with NaCl saline on both sides of the preparation, generated a V_{te} of $+0.8 \pm 0.4$ mV ($N = 3$) when symmetrically perfused with NaCl saline. Short-circuiting resulted in an I_{sc} of $-5 \pm 3\,\mu A\,cm^{-2}$ with a G_{te} of $4.2 \pm 1.9\,mS\,cm^{-2}$. Like the midgut, omission of external glucose or addition of external amino acids did not affect the electrophysiological parameters of the tissue. Na^+- or Cl^--free salines did not produce significant currents requiring further analysis.

The ionic permeabilities of this hindgut tissue are shown in Figure 3. The mean permeability sequence was $NO_3^- \cong Cl^- \gg K^+ > Na^+ \cong CH_3COO^- \cong$ gluconate $> SO_4^{2-} \cong Ca^{2+} \cong Mg^{2+}$. The $P_{Cl^-}:P_{Na^+}$ ratio of 4.1 reveals marked anion selectivity.

The estuarine crab, Chasmagnathus granulata, adapted to 2‰ salinity

Micro-anatomy

In *C. granulata*, the midgut epithelium consists of a simple cell layer of 80–100 μm thickness, deeply folded into crypts (Fig. 4A). The predominant tall, narrow columnar cells display apical microvilli above a thin, dense cytoplasmic layer, and a large, lightly staining, elliptical, medial nucleus in a uniform, slightly vesiculated cytoplasm. The epithelium lies on a thin, dense, highly

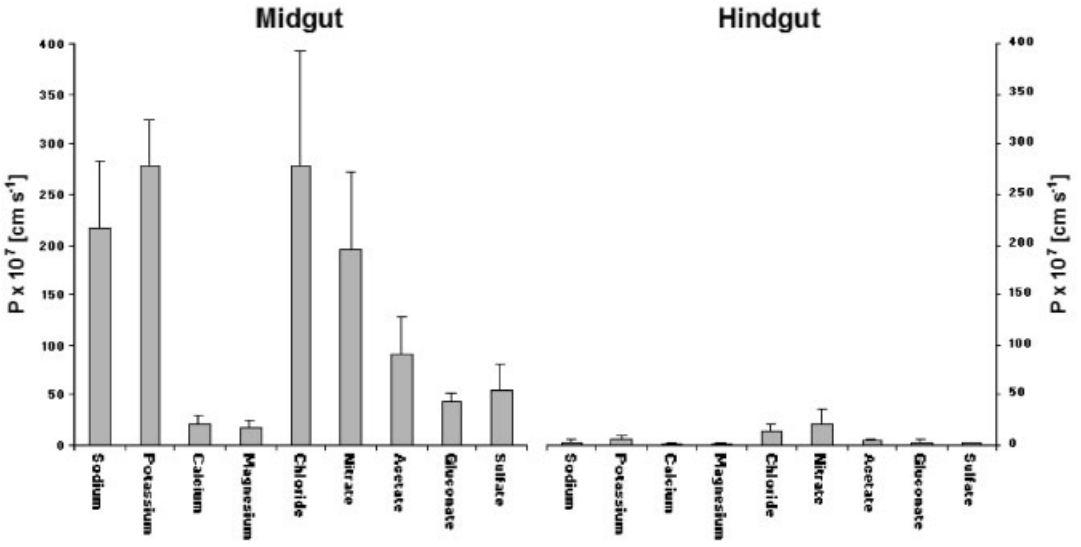

Fig. 3. Ionic permeabilities (mean ± SEM) of the mid- and hindguts of *Sesarma rectum* adapted to 15‰ salinity. K^+, Cl^-, Na^+ and NO_3^- permeabilities are highest in the midgut, with NO_3^- in the hindgut. Both segments show low permeability to Ca^{2+} and Mg^{2+}.

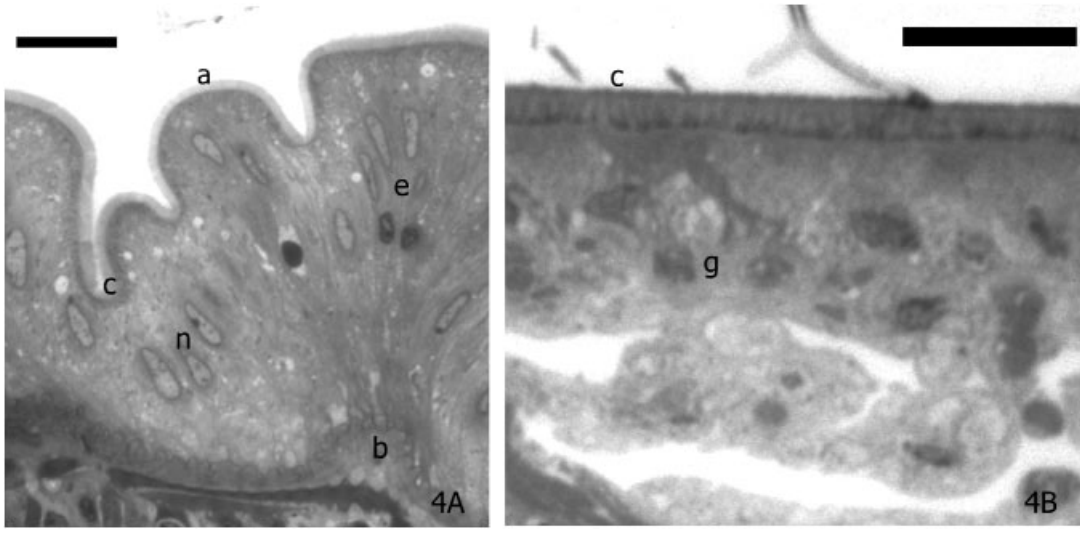

Fig. 4. Micro-anatomy of the mid- and hindguts of the estuarine crab, *Chasmagnathus granulata*, adapted to 2‰ salinity. (**A**) Midgut wall showing a monolayer of very tall, columnar epithelial cells (e) with apical microvilli (a) and medially located nuclei (n), deeply folded into crypts (c), overlying a well-developed, folded basement membrane (b). (**B**) Hindgut, revealing a single layer of globular, subspherical epithelial cells (g) with mainly basal nuclei, overlain by a thin cuticle (c). Scale bars = 20 μm.

folded basement membrane overlying a dense basement lamina.

The thin (60 μm) hindgut epithelium (Fig. 4B) is overlain by a fine, 10-μm-thick cuticle, and underlain by a fibrous basal lamina, penetrated by wide intercellular spaces. The constituent cells are subspherical, and possess an unvesiculated, apically dense cytoplasm with mainly basal nuclei.

Electrophysiology

Midgut tissue sheets from *C. granulata*, mounted in the Ussing-type chamber and perfused

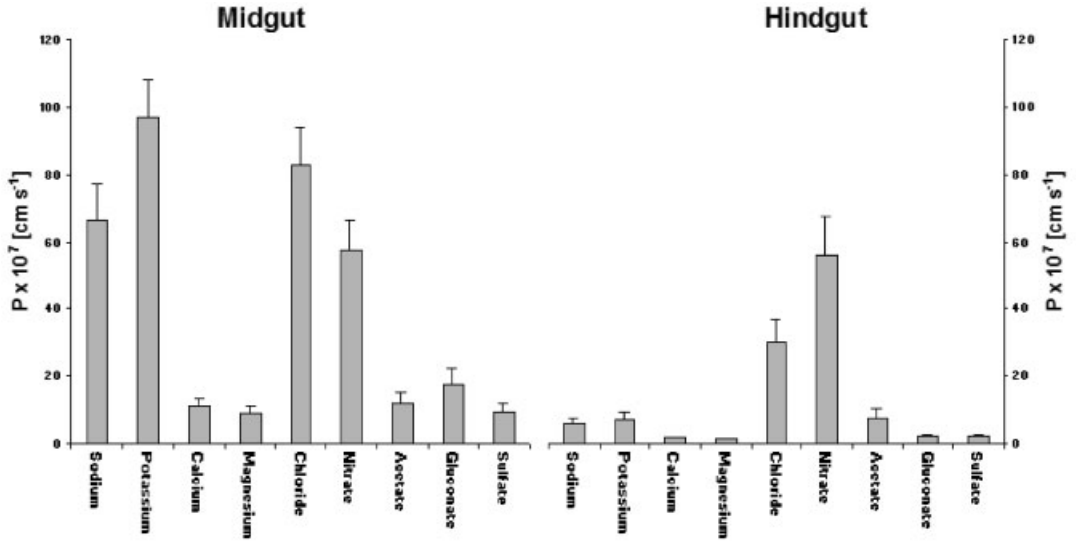

Fig. 5. Ionic permeabilities (mean ± SEM) of the mid- and hindguts of *Chasmagnathus granulata* adapted to 2‰ salinity. K^+, Cl^-, Na^+ and NO_3^- permeabilities predominate in the midgut, with NO_3^- in the hindgut. The hindgut shows low permeability to Ca^{2+} and Mg^{2+}.

on both sides with hemolymph-like NaCl saline, produced a V_{te} of -0.5 ± 0.3 mV ($N = 5$). Short circuiting resulted in an I_{sc} of $+12 \pm 10\ \mu A\,cm^{-2}$ with a G_{te} of $42 \pm 10\ mS\,cm^{-2}$. Neither omission of external glucose nor addition of external amino acids affected I_{sc} or G_{te}. Symmetrically perfused Na^+- or Cl^--free salines did not produce short-circuit currents indicative of active ion transport.

The ionic permeabilities of this midgut tissue are given in Figure 5. The mean permeability sequence was $Cl^- \cong K^+ > Na^+ \cong NO_3^- >$ gluconate $> CH_3COO^- \cong SO_4^{2-} \cong Ca^{2+} \cong Mg^{2+}$, very similar to *S. rectum*. The P_{Cl^-}:P_{Na^+} ratio of 1.2 discloses no significant anion or cation selectivity.

Hindgut tissue produced a V_{te} of $+1.5 \pm 0.5$ mV ($N = 4$) when perfused on both sides with hemolymph-like NaCl saline. Short circuiting generated an I_{sc} of $-11 \pm 3\ \mu A\,cm^{-2}$ with a transepithelial conductance of $7.0 \pm 0.9\ mS\,cm^{-2}$. Again, omission of external glucose or addition of external amino acids did not affect these parameters, and the symmetrical perfusion of Na^+- or Cl^--free salines did not produce significant currents requiring further analysis.

The ionic permeabilities of this hindgut tissue are summarized in Figure 5. The mean ion permeability sequence was $NO_3^- \cong Cl^- > K^+ \cong CH_3COO^- \cong Na^+ >$ gluconate $\cong SO_4^{2-} \cong Ca^{2+} \cong Mg^{2+}$, very similar to *S. rectum*. The P_{Cl^-}:P_{Na^+} ratio of 5.4 reveals marked anion selectivity.

The hololimnetic, freshwater crab, Dilocarcinus pagei

Micro-anatomy

Light microscopic analysis of transverse epoxy sections through the presumptive thoracic midgut of *D. pagei* revealed an irregular epithelium of 20–100 μm thickness, overlain by a heavy, 50-μm-thick cuticle (Fig. 6A). The epithelial cells are squat to columnar, lack apical microvilli, and exhibit a dense, apical cytoplasm with a medial, darkly staining, elliptical nucleus; the basal cytoplasm is slightly vesiculated. Tegumental glands are present in the basal lamina. Such a micro-anatomy is typical of the brachyuran hindgut, which evidently penetrates into the thoracic cavity in *D. pagei*.

The abdominal hindgut epithelium of *D. pagei* consists of columnar cells about 40 μm in height, with semispherical to elongate, basal nuclei, lying on a fine, convoluted basement membrane, and is overlain by a thin (15 μm) cuticle (Fig. 6B). The narrow band of apical cytoplasm is notably dense, tubular and unvesiculated while the remaining cytoplasm is markedly vesiculated. Longitudinal, striated, muscle fiber blocks and tegumental glands are present in the basal lamina.

Scanning electron microscopy of the thoracic (anterior) hindgut in *D. pagei* reveals a highly folded, cuticular lining (Fig. 7A) with numerous, frequently overlapping, raised, fanlike scales,

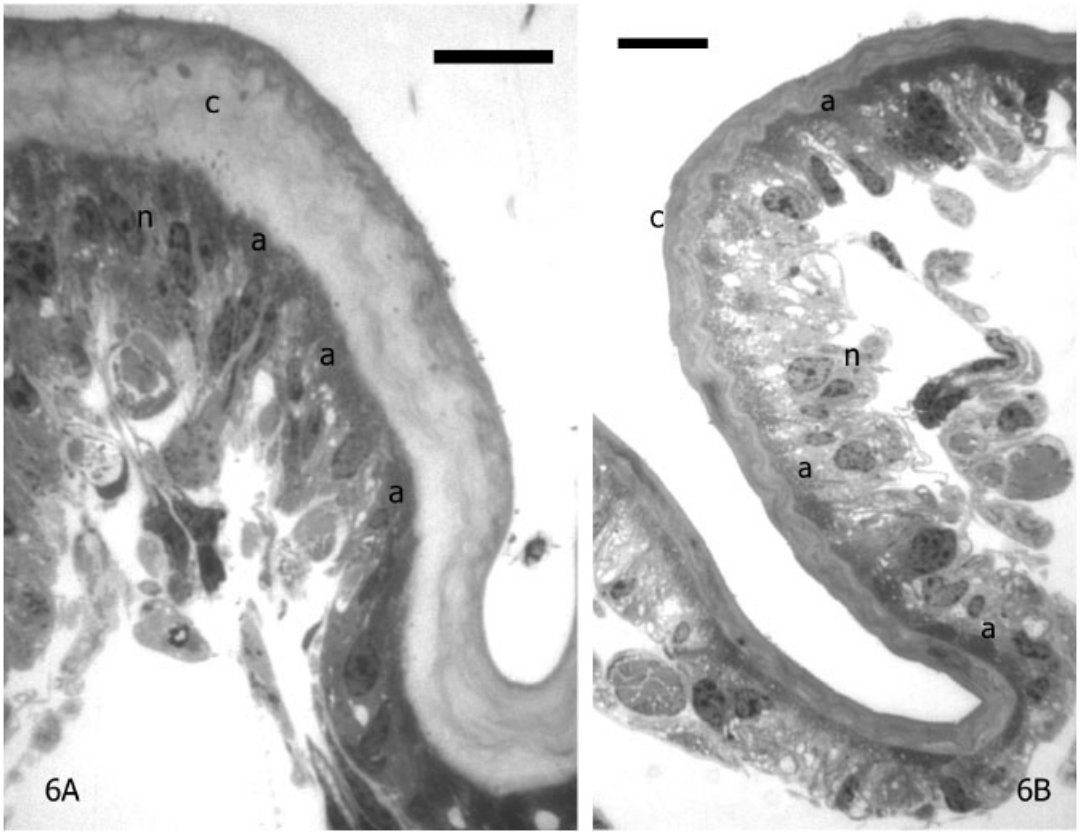

Fig. 6. Micro-anatomy of the thoracic (anterior) and abdominal (posterior) hindguts of the freshwater crab *Dilocarcinus pagei*. (**A**) Thoracic (anterior) hindgut showing heavy cuticle (c) and squat, irregular epithelial cells with dense apical cytoplasm (a) and medially located nuclei (n). (**B**) Abdominal (posterior) hindgut with fine cuticle (c), showing a monolayer of columnar epithelial cells with dense, homogeneous, apical cytoplasm (a), vesicular medial cytoplasm and basal nuclei (n). Scale bars = 20 μm.

exhibiting 5-μm-long spiny setae on the posterior-pointing edge (Fig. 7B). Patchy, bare areas lacking scales are often present.

The cuticular lining of the abdominal (posterior) hindgut is less folded, presenting long, open plicae (Fig. 7C), which exhibit abundant, close-packed, flattish scales with posterior-pointing setae (Fig. 7D), often organized into regular rows.

Electrophysiology

A V_{te} of -2.2 ± 0.4 mV ($N = 5$) was recorded on symmetrically perfusing the thoracic (anterior) hindgut tissue preparation of *D. pagei* with hemolymph-like NaCl saline. Short-circuiting V_{te} resulted in an I_{sc} of $+0.7 \pm 0.1\ \mu A\,cm^{-2}$ with a G_{te} of $0.4 \pm 0.1\ mS\,cm^{-2}$. Omission of external glucose did not affect I_{sc} or G_{te}. Addition of external arginine, lysine or valine ($1\ mmol\,l^{-1}$) did not alter these parameters; Na^+- or Cl^--free salines perfused on both sides of the preparation did not generate currents reflecting active ion transport.

The ionic permeabilities of the anterior hindgut tissue are summarized in Figure 8. The mean ion permeability sequence was $K^+ \cong Na^+ > NO_3^- \cong Cl^- > Ca^{2+} \cong$ gluconate $\cong Mg^{2+} > SO_4^{2-} \cong CH_3COO^-$. The $P_{Cl^-}:P_{Na^+}$ ratio of 0.23 reveals marked cation selectivity.

The abdominal (posterior) hindgut tissue generated a V_{te} of -2.7 ± 0.9 mV ($N = 5$) when symmetrically perfused with NaCl saline. Short circuiting produced an I_{sc} of $+2.4 \pm 1.3\ \mu A\,cm^{-2}$ with a G_{te} of $0.7 \pm 0.3\ mS\,cm^{-2}$. As seen in the thoracic hindgut, omission of external glucose or addition of external amino acids did not affect the electrophysiological parameters of this tissue. Na^+- or Cl^--free salines did not produce significant currents requiring further analysis.

The ionic permeabilities of the posterior hindgut tissue are given in Figure 8. The mean ion permeability sequence of $NO_3^- > Cl^- > CH_3COO^- > Na^+$

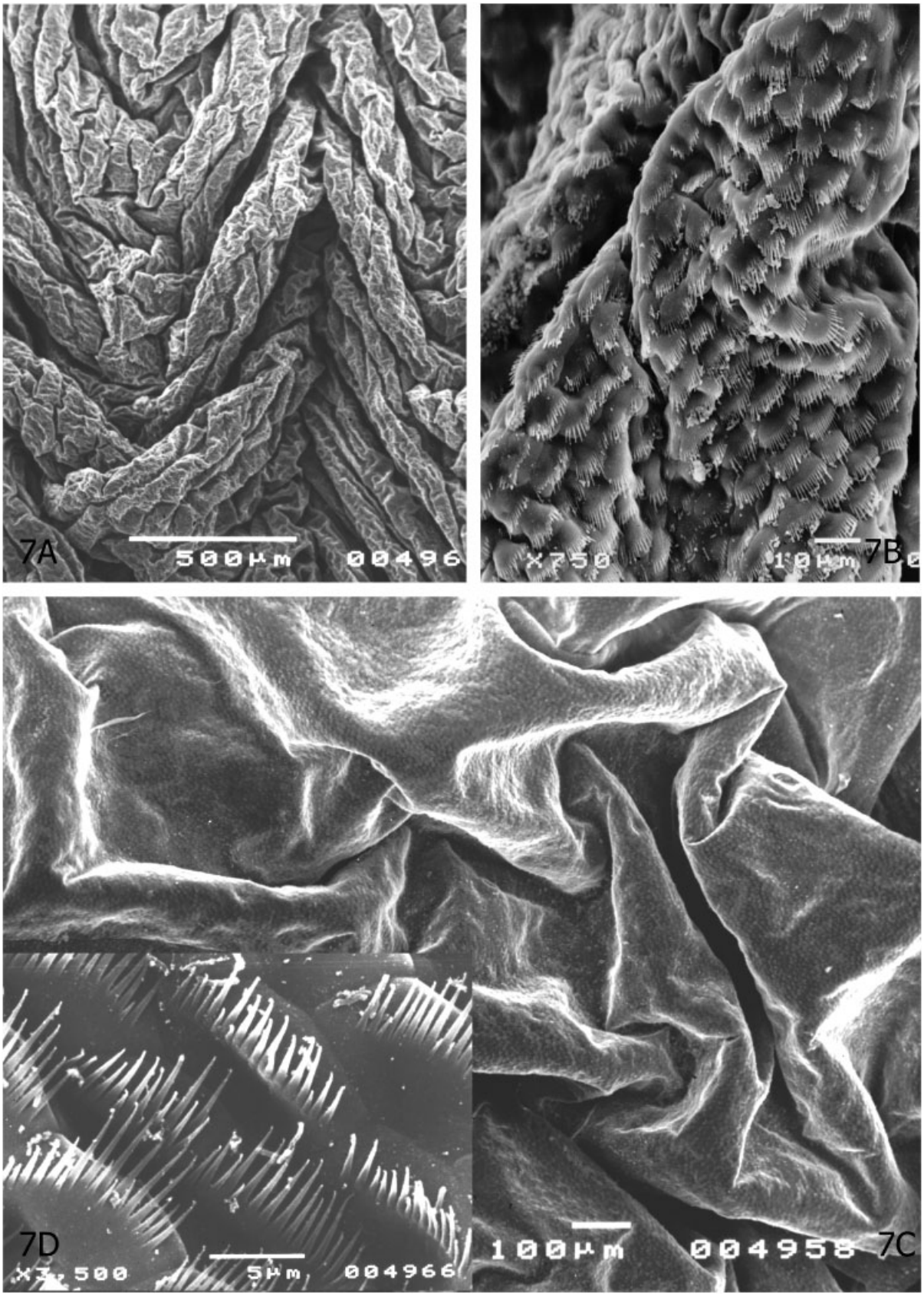
7A
500µm
00496
X750
10µm
7B
7D
X3,500
5µm
004966
100µm
004958
7C

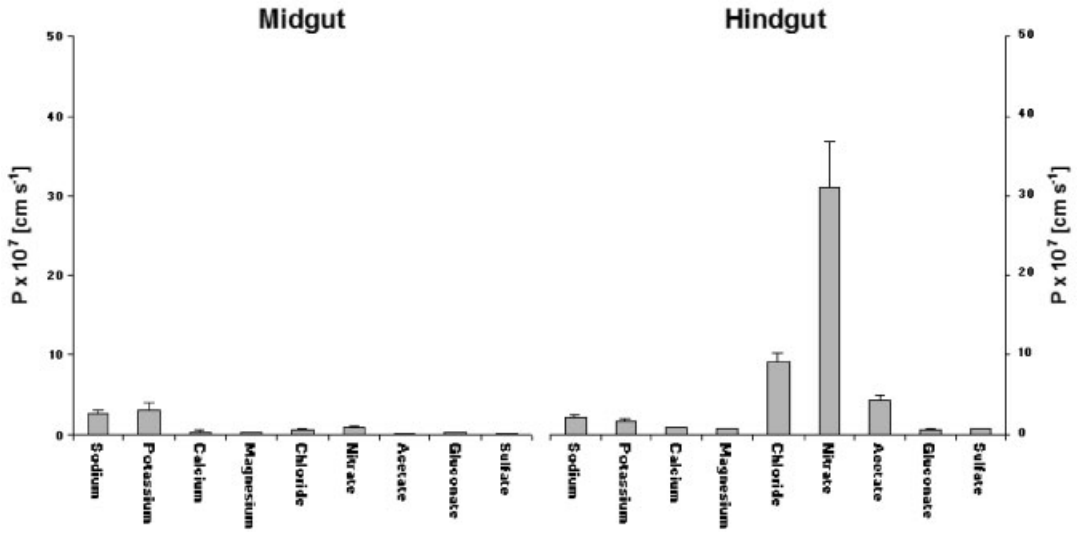

Fig. 8. Ionic permeabilities (mean ± SEM) of the thoracic and abdominal hindguts of the freshwater crab *Dilocarcinus pagei*. While the thoracic hindgut is almost impermeable, the abdominal hindgut is permeable to NO_3^-.

$\cong K^+ > \cong Ca^{2+} \cong Mg^{2+} \cong SO_4^{2-} \cong$ gluconate is similar to those for *S. rectum* and *C. granulata*, as is the pronounced anion selectivity for this gut region ($P_{Cl^-}:P_{Na^+} = 4.1$).

DISCUSSION

Micro-anatomy

The midguts of the crabs inhabiting saline waters (*C. granulata* and *S. rectum*) consist of a monolayer of tall, columnar epithelial cells, with apical microvilli and medially located nuclei, overlying a well-developed, folded basement membrane, features typical of a transporting epithelium (Mykles, '79). Interestingly, the corresponding gut region in *D. pagei*, the freshwater species, is cuticle lined, lacks microvilli, is composed of squat epithelial cells, and thus constitutes a thoracic or anterior portion of the hindgut. The patchiness of the cuticular scales in this segment suggests a transition zone to the midgut, evidently very reduced in this hololimnetic crab. The hindguts in all three crabs are cuticle lined, and no specific adaptations for transepithelial transport, like apical or basal membrane areas increased by microvilli or infoldings, are visible by light microscopy in the epithelial cells. The thick layer of circular and longitudinal muscle fiber blocks, together with the posterior-pointing, spiny scales suggest a predominant role in the mechanical transport of the gut contents along the intestinal tube.

Nutrient absorption

Nutrient absorption is the predominant role of the intestinal tract in animals, and is often accomplished by separate parts of the digestive system after mechanical and enzymatic breakdown of the food particles.

The midgut/thoracic hindgut epithelia of all three crabs, and the abdominal (posterior) hindgut of *D. pagei*, exhibit similar ($P > 0.05$), small, lumen-negative, transepithelial voltages when identical hemolymph-like salines are perfused on both sides. The hindgut preparations of the salt-water-inhabiting species (*C. granulata* and *S. rectum*) displayed similar ($P > 0.05$), small voltages of opposite polarity. After voltage clamping, very small short-circuit currents (I_{sc}) were

Fig. 7. Scanning electron microscopy of the intestinal lumen of the freshwater crab *Dilocarcinus pagei*. (**A**) Cuticle-lined, thoracic (anterior) hindgut surface, showing numerous, shallow regular folds (scale bar = 0.5 μm). (**B**) Detail of characteristic, scaly, thoracic (anterior) hindgut lining, with profuse, regularly arranged, posterior-pointing, spiny scales (scale bar = 10 μm). (**C**) Cuticle-lined, scaly, abdominal (posterior) hindgut surface showing long, open, deep irregular folds (scale bar = 100 μm). (**D**) Detail of luminal abdominal (posterior) hindgut surface, showing regularly arranged rows of scales with numerous, long, posterior-pointing setae (scale bar = 5 μm).

detected. The similar ($P > 0.05$) positive currents (corresponding to the luminally negative voltages in the three midgut/thoracic hindgut sections, and in the abdominal hindgut of *D. pagei*) may suggest active, Na^+-coupled glucose or amino acid absorption. However, the omission of luminal glucose did not reduce I_{sc}, suggesting that this current does not reflect Na^+-coupled glucose transport. The addition of three essential amino acids to the luminal bath did not alter I_{sc}, contrasting with previous reports of Na^+-coupled glycine and glucose absorption by marine and freshwater shrimp midguts (Ahearn, '74, '76; Ahearn and Maginniss, '77).

These data suggest that active, electrogenic nutrient absorption is either absent, undetectable using the present techniques, or rather, electrically neutral, and thus ''invisible'' to our electrophysiological techniques. Na^+/glucose transport is, however, electrogenic in lobsters (Reshkin et al., '88) and rats (Wright, 2000), while the transport of amino acids like glutamate and leucine is electrically neutral (Reshkin et al., '88). Further, active, electrogenic transport of nutrients may be hormonally triggered, a capability abolished after isolation of the epithelium from the circulation. Crustacean hyperglycemic hormone, for example, regulates glucose levels (Santos and Keller, '93), and midgut and hindgut endocrine cells produce this hormone during late pre-molt (Chung et al., '99). Other hormones such as insulin-like growth factors decrease glucose levels in crustacean hemolymph (Verri et al., 2001), and other factors originating in the crustacean eyestalk neurosecretory system inhibit lipid synthesis (O'Connor and Gilbert, '68). Evidently, a large number of hormones modulate feeding-related events in the Crustacea. In some experiments, we employed theophylline, a phosphodiesterase inhibitor that increases cytosolic cyclic AMP by inhibiting its degradation to 5′-AMP (Johnsen and Nielsen, '78). However, there was no effect on transepithelial currents or conductances (data not shown). Nevertheless, hormonally triggered, nutrient transport may yet be present in the midgut epithelia studied here.

Ion transport

Ion transport is a well-known capability of intestinal epithelia, and in many animals, the intestine is the only body surface available for water and ion absorption. For example, certain gut segments or diverticula like the insect Malpighian tubule or elasmobranch rectal gland are involved in osmotic and ionic regulation (Linton and O'Donnell, '99). In the Crustacea, organisms possessing a calcium-rich exoskeleton, the digestive system, particularly the cardiac stomach, plays a prominent role in calcium recovery and storage from the previous exoskeleton during premolt (Greenaway, '85).

The low positive currents found here in the midgut/thoracic hindgut epithelia may reflect some degree of active, electrogenic Ca^{2+} absorption. However, perfusion with Ca^{2+}-free saline did not reduce these currents in preliminary experiments (data not shown). Further, the mid- and hindgut epithelial permeabilities for Ca^{2+} are low. We used intermolt animals exclusively, however, and molting crabs might show greater Ca^{2+} currents. For example, active Ca^{2+} reabsorption via the gills increases significantly during postmolt (Greenaway, '85), and a similar phenomenon may occur in the midgut/thoracic hindgut. The gut epithelia examined also showed no signs of active, electrogenic Na^+ and/or Cl^- transport. The short-circuit currents measured with hemolymph-like NaCl saline on both sides of the epithelium were very small, and ion substitution experiments did not disclose the absorption or secretion of Na^+ and/or Cl^- ions. However, all three crabs are good hyperosmoregulators and maintain differential osmotic and ionic gradients across their body surfaces. Chu ('87) also reported very small transmural potential differences in gut segments of the blue crab, a strong osmoregulator, and suggested that the gut was an unlikely route for ion regulation. However, an electrical potential difference across the midgut as a result of net, transmural Na^+, Cl^- and K^+ movements has been found in freshwater prawns (Ahearn and Maginniss, '77; Ahearn, '80).

Another well-known transport capacity shown by the crustacean midgut is fluid absorption during pre-molt prior to ecdysis. In the American lobster, *Homarus americanus*, non-electrogenic fluid absorption occurs in the absence of an osmotic gradient, indicating that it may be driven by NaCl absorption (Mykles, '80). Such fluid absorbtion by the midgut, probably as a result of permeability changes (Mykles and Ahearn, '78), leads to hydration and swelling, culminating in hormonally regulated ecdysis. However, in the present study, we examined the gut segments of intermolt crabs, which exhibit little or negligible fluid absorption. It would be of considerable interest to investigate the mechanism of the NaCl

absorption that drives fluid absorption at ecdysis. With regard to nutrient absorption (see above), note that the techniques employed here detect only electrogenic transport. Since a role for electroneutral ion transport in the crustacean midgut cannot be excluded, future studies should utilize electrophysiological techniques simultaneously with tracer flux measurements.

Although the regulation of passive salt losses by active absorption seems to be restricted to the gill epithelia in most crustaceans, the conductances of the gut segments and their ionic permeabilities do reflect certain adaptations to osmotic challenge. The midguts of the saltwater-inhabiting species exhibit similar ($P > 0.05$), elevated transepithelial conductances, significantly greater ($P < 0.001$) than that of the freshwater dweller, but no particular cation or anion selectivity (see Results and Figs. 3 and 5). Hindgut conductance in the saltwater species is significantly less ($P \leq 0.004$), with moderate anion selectivity. Apparently, ions are quite freely exchanged across the midgut epithelia, while the reduced conductances and the ion selectivities of the hindguts may prevent major ion losses. The freshwater species, *D. pagei*, however, exhibits a very different behavior: the thoracic (anterior) and abdominal (posterior) hindgut epithelia show similar ($P = 0.37$), very low conductances, and are ion selective (see results and Fig. 8). Both these characteristics diminish passive salt losses since reduced conductance hinders passive ion movement down a concentration gradient. Similar changes in passive permeability of the midgut are seen when *Callinectes* is acclimated to dilute media, particularly for Na^+ ions (Chu, '87). Further, the passive, ionic permeability sequence for freshwater prawn midgut is $P_{K^+} = 5.1 < P_{Na^+} = 1.0 < P_{Cl^-} = 0.5$ (Ahearn, '80).

The ionic permeabilities disclosed in the present investigation were established using an electrophysiological technique, and thus do not reflect putative, electroneutral, transcellular pathways. Since active, electrogenic transport is very diminished or absent from these epithelia, such permeabilities most likely reflect paracellular pathways, which include the cuticle where present, rather than a transcellular route. Relatively high permeabilities were revealed for K^+ ions in the midguts/thoracic hindgut, and for NO_3^- in the hindguts, and a low concentration of both of these ions compared to Na^+ and Cl^-, respectively, can be assumed in the hemolymph and hindgut lumen. Thus, these high K^+ and NO_3^- permeabilities appear to be of minor physiological importance, apparently reflecting the physical characteristics of the permeability barriers.

The conductance and ion permeabilities of the gut cuticles were not examined separately in the present study. Thus, the reduced conductances and ion selectivities may derive from both the cuticle and/or the underlying epithelium. The conductance and permeability of crustacean gill cuticles have been investigated in crabs and crayfish (Avenet and Lignon, '85; Lignon, '87; Lignon and Péqueux, '90). Such studies show that gill cuticle conductance and ion selectivity are lower in freshwater than saltwater-inhabiting species (Lignon and Péqueux, '90). However, the conductance of the crustacean gill cuticle is much greater than those found here for cuticle-lined gut epithelia. In the gills, resistance is mainly due to the underlying epithelium (Onken and McNamara, 2002; Onken and Riestenpatt, 2002). Even so, a detailed investigation of the gut cuticle in crabs confronting different osmotic challenges would be of interest.

The present study shows that the mid- and hindguts of marine and freshwater crabs are fairly inactive electrically, and that active, electrogenic transport of nutrients is apparently undetectable electrophysiologically. The principal role of these gut segments appears to be the mechanical transport of pre-digested material to the rectum. The micro-anatomical features disclosed, however, do suggest ion/nutrient transport by the midgut epithelia of *C. granulata* and *S. rectum*, and these epithelia are thus candidates for future studies of hormonally triggered nutrient absorption. Our findings are consistent with those of earlier studies, showing that most nutrients seem to be absorbed via the hepatopancreas (Ahearn et al., '85, '87, '90, '99; Ahearn and Clay, '89; Ahearn, '96). Thus far, the transport characteristics of the hepatopancreas have been studied almost entirely at the cellular level (Ahearn et al., '94, 2001; Ahearn and Zhuang, '96; Zhuang and Ahearn, '98). The use of isolated and perfused hepatopancreas tubules would be convenient to better understand the transport characteristics of this organ.

Although active salt absorption was not detected, the osmoregulatory capability of the crabs studied is clearly reflected in the conductances and ion permeabilities of their gut epithelia, particularly in finding, in the red freshwater crab, *D. pagei*, a cuticle-lined, thoracic (anterior) hindgut epithelium in a region in which the midgut might

be expected. In the saltwater inhabitants (*S. rectum* and *C. granulata*), the midgut epithelium has a high conductance but no significant ion selectivity. Since no active salt absorption was detected in the hindguts, significant salt losses may occur via this route, despite the reduced conductance and marked anion selectivity. However, active salt absorption by the hindgut may be hormonally triggered in hyperosmoregulating crabs, and thus not detected in the present study. A more detailed investigation to disclose whether putative, hormonally stimulated, active salt absorption and water movements take place in the hindgut and posterior ceca of such Crustacea would certainly be useful.

ACKNOWLEDGMENTS

This study was supported by research grants from the Fundação de Amparo à Pesquisa do Estado de São Paulo, Brazil (FAPESP 1998/09756-9) to F.P.Z., and the Deutscher Akademischer Austauschdienst (DAAD/GTZ) Germany to H.O. and J.C.M. HO acknowledges research support through a Visiting Professorship from CAPES(Brazil)/DAAD, and J.C.M. a research scholarship from the Conselho Nacional de Desenvolvimento Científico e Tecnológico (CNPq 303282/84-3). We thank Dr. M.L. Negreiros-Fransozo (UNESP, Botucatu) for providing *Sesarm rectum* and *Chasmagnathus granulata*.

LITERATURE CITED

Ahearn GA. 1974. Kinetic characteristics of glycine transport by the isolated midgut of the marine shrimp, *Penaeus marginatus*. J Exp Biol 61:677–696.

Ahearn GA. 1976. Co-transport of glycine and sodium across the mucosal border of the midgut epithelium in the marine shrimp, *Penaeus marginatus*. J Physiol 258:499–520.

Ahearn GA. 1978. Allosteric cotransport of sodium, chloride and calcium by the intestine of freshwater prawns. J Memb Biol 42:281–300.

Ahearn GA. 1980. Intestinal electrophysiology and transmural ion transport in freshwater prawns. Am J Phys 239:1–10.

Ahearn GA. 1996. The invertebrate electrogenic $2Na^+/1H^+$ exchanger: polyfunctional epithelial workstation. News Physiol Science 11:31–35.

Ahearn GA, Clay LP. 1989. Kinetic analysis of electrogenic $2Na^+$–$1H^+$ antiport in crustacean hepatopancreas. Am J Phys 257:484–493.

Ahearn GA, Franco P. 1990. Sodium and calcium share the electrogenic $2Na^+$–$1H^+$ antiporter in crustacean antennal glands. Am J Phys 259:758–767.

Ahearn GA, Franco P. 1993. Ca^{2+} transport pathways in brush-border membrane vesicles of crustacean antennal glands. Am J Phys 264:1206–1213.

Ahearn GA, Maginniss LA. 1977. Kinetics of glucose transport by the perfused mid-gut of the freshwater prawn *Macrobrachium rosenbergii*. J Physiol 271:319–336.

Ahearn GA, Zhuang Z. 1996. Cellular mechanisms of calcium transport in crustaceans. Phys Zool 69:383–402.

Ahearn GA, Grover ML, Dunn RE. 1985. Glucose transport by lobster hepatopancreatic brush-border membrane vesicles. Am J Phys 248:R133–R141.

Ahearn GA, Grover ML, Dunn RE. 1986. Effects of Na^+, H^+, and Cl^- on alanine transport by lobster hepatopancreatic brush border membrane vesicles. J Comp Physiol 156B:537–548.

Ahearn GA, Grover ML, Tsuji RT, Clay LP. 1987. Proton-stimulated $Cl^-/HCO3^-$ antiport by basolateral membrane vesicles of lobster hepatopancreas. Am J Phys 252:859–870.

Ahearn GA, Franco P, Clay LP. 1990. Electrogenic $2Na^+/1H^+$ exchange in crustaceans. J Memb Biol 116:215–226.

Ahearn GA, Zhuang Z, Duerr J, Pennington V. 1994. Role of the invertebrate electrogenic $2Na^+/1H^+$ antiporter in monovalent and divalent cation transport. J Exp Biol 196: 319–335.

Ahearn GA, Duerr JM, Zhuang Z, Brown RJ, Aslamkhan A, Killebrew DA. 1999. Ion transport processes of crustacean epithelial cells. Phys Biochem Zool 72:1–18.

Ahearn GA, Mandal PK, Mandal A. 2001. Biology of the $2Na^+/1H^+$ antiporter in invertebrates. J Exp Zool 289:232–244.

Avenet P, Lignon JM. 1985. Ionic permeabilities of the gill lamina cuticle of the crayfish, *Astacus leptodactylus* (E). J Physiol 363:377–401.

Bond-Buckup G, Buckup L, Fontoura NF, Marroni NP, Kucharski LC. 1991. O caranguejo: manual para o ensino prático em Zoologia. Porto Alegre: Editora da Universidade Federal de Rio Grande do Sul. 71 p.

Bromberg E, Santos EA, Bianchini A. 1995. Osmotic and ionic regulation in Chasmagnathus granulata Dana, 1951 (Decapoda, Grapsidae) during hyposmotic stress. Nauplius 3:83–99.

Brunet M, Arnaud J, Mazza J. 1994. Gut structure and digestive cellular processes in marine Crustacea. Oceanogr Mar Biol 32:335–367.

Chu KH. 1987. Sodium transport across the perfused midgut and hindgut of the blue crab, *Callinectes sapidus*: the possible role of the gut in crustacean osmoregulation. Comp Biochem Physiol 87A:21–25.

Chung JS, Dircksen H, Webster SG. 1999. A remarkable, precisely timed release of hyperglycemic hormone from endocrine cells in the gut is associated with ecdysis in the crab *Carcinus maenas*. Proc Natl Acad Sci 96:13103–13107.

Clark TM, Koch A, Moffett DF. 2000. The electrical properties of the anterior stomach of the larval mosquito (Aedes aegypti). J Exp Biol 203:1093–1101.

Cuzon G, Guillaume J, Cahu C. 1994. Composition, preparation and utilization of feeds for Crustacea. Aquaculture 124:253–267.

Dall W, Moriarty DJW. 1983. Functional aspects of nutrition and digestion. In: Bliss DE, editor. The biology of Crustacea, Vol. 5, Mantel LH, editor. Internal anatomy and physiological regulation. New York: Academic Press. p 215–261.

D'Incao F, Ruffino ML, Silva KG, Braga AC. 1992. Responses of *Chasmagnathus granulata* Dana (Decapoda: Grapsidae) to salt-marsh environmental variations. J Exp Mar Biol Ecol 161:179–188.

Dow JAT. 1981. Countercurrent flows, water movements and nutrient absorption in the locust midgut. J Insect Physiol 27:579–585.

Flik G, Verbost PM, Atsma W, Lucu C. 1994. Calcium transport in gill plasma membranes of the crab *Carcinus maenas*: evidence for carriers driven by ATP and a Na^+ gradient. J Exp Biol 195:109–122.

Greenaway P. 1985. Calcium balance and moulting in the Crustacea. Biol Review 60:425–454.

Herrera-Alvarez L, Fernandez I, Benito J, Pardos F. 2000. Ultrastructure of the midgut and hindgut of *Derocheilocaris remanei* (Crustacea, Mystacocarida). J Morphol 244: 177–189.

Hodgkin AL, Horowitz P. 1959. The influence of potassium and chloride ions on the membrane potential of single muscle fibers. J Physiol 148:127–160.

Icely JD, Nott JA. 1992. Digestion and absorption: digestive system and associated organs. In: Harrison FW, editor. Microscopic anatomy of invertebrates, Vol. 10, Harrison FW, Hume AG, editors. Decapod Crustacea. New York: Wiley-Liss. p 147–201.

Johnsen AH, Nielsen R. 1978. Effects of antidiuretic hormone, arginine vasotocin, theophylline, fillipin and A23187 on cyclic AMP in isolated frog skin epithelium (*R. temporaria*). Acta Physiol Scand 102:281–289.

Lignon JM. 1987. Ionic permeabilities of the isolated gill cuticle of the shore crab *Carcinus maenas*. J Exp Biol 131:159–174.

Lignon JM, Péqueux A. 1990. Permeability properties of the cuticle and gill ion exchanges in decapod crustaceans. In: Mellinger J, Truchot JP, Lahlou B, editors. Comparative physiology, Vol. 6, Animal nutrition and transport processes. 2, Transport, respiration and excretion: comparative and environmental aspects. Basel: Karger. p 14–27.

Linton SM, O'Donnell MJ. 1999. Contributions of K^+:Cl^- cotransport and Na^+/K^+-ATPase to basolateral ion transport in Malpighian tubules of *Drosophila melanogaster*. J Exp Biol 202:1561–1570.

Lucu C. 1993. Ion transport in the gill epithelium of aquatic Crustacea. J Exp Zool 265:378–386.

Mantel LH, Farmer LL. 1983. Osmotic and ionic regulation. In: Bliss DE, editor. The biology of Crustacea, Vol. 5, Mantel LH, editor. Internal anatomy and physiological regulation. New York: Academic Press. p 53–161.

Mu YY, Shim KF, Guo JY. 1998. Effects of protein level in isocaloric diets on growth performance of the juvenile Chinese hairy crab, *Eriocheir sinensis*. Aquaculture 165: 139–148.

Mykles DL. 1979. Ultrastructure of alimentary epithelia of lobsters, *Homarus americanus* and *H*. gammarus, and crab Cancer magister. Zoomorphologie 92:201–215.

Mykles DL. 1980. The mechanism of fluid absorption at ecdysis in the American lobster, *Homarus americanus*. J Exp Biol 84:89–101.

Mykles DL, Ahearn GA. 1978. Changes in fluid transport across the perfused midgut of the freshwater prawn, *Macrobrachium rosenbergii,* during the molting cycle. Comp Biochem Physiol 61A:643–645.

O'Connor JD, Gilbert LI. 1968. Aspects of lipid metabolism in crustaceans. Am Zool 8:529–539.

Onken H, McNamara JC. 2002. Hyperosmoregulation in the red freshwater crab *Dilocarcinus pagei* (Brachyura, Trichodactylidae): structural and functional asymmetries of the posterior gills. J Exp Biol 205:167–175.

Onken H, Riestenpatt S. 2002. Ion transport across posterior gills of hyper-osmoregulating shore crabs (*Carcinus maenas*): amiloride blocks the cuticular Na^+ conductance and induces current-noise. J Exp Biol 205:523–531.

Reshkin SJ, Cassano G, Womersley C, Ahearn GA. 1988. Preservation of glucose transport and enzyme activity in fish intestinal brush-border and basolateral membrane vesicles. J Exp Biol 140:123–135.

Santos EA, Keller R. 1993. Regulation of circulating levels of the crustacean hyperglycemic hormone: evidence for a dual feedback control system. J Comp Physiol 163B:374–379.

Verri T, Mandal A, Zilli L, Bossa D, Mandal PK, Ingrosso L, Zonno V, Vilella S, Ahearn GA, Storelli C. 2001. D-glucose transport in decapod crustacean hepatopancreas. Comp Biochem Physiol 130A:585–606.

Wright EM, Loo DD. 2000. Coupling between Na^+, sugar, and water transport across the intestine. Ann N Y Acad Sci 915:54–66.

Yonge CM. 1924. Studies on the comparative physiology of digestion. II. The mechanism of feeding, digestion, and assimilation in *Nephrops norvegicus*. J Exp Biol 1:343–390.

Zanotto FP. 2000. Nutritional requirements in Brachyura: a review. Nauplius 8:107–111.

Zhuang Z, Ahearn GA. 1998. Energized Ca^{2+} transport by hepatopancreatic basolateral plasma membranes of *Homarus americanus*. J Exp Biol 201:211–220.